On the Applied Efficiency of Systematic Earthquake Prediction

V. G. Gitis, A. B. Derendyaev(✉), and K. N. Petrov

The Institute for Information Transmission Problems, Moscow, Russia
gitis@iitp.ru, wintsa@gmail.com, stranger12@list.ru

Abstract. The systematic forecast of earthquakes is regularly performed with a step of Δt in a predetermined analysis zone. At each step, the training set of target earthquakes is augmented, new data about the seismic process is loaded, the data is processed, transformed into grid-based fields, and the machine learning program calculates a solution using all available data from the beginning of the training to the moment t^* of the earthquake forecast. The result is a map of the alarm zone in which the epicenter of the target earthquake is expected in the interval $(t^*, t^* + \Delta t]$. At the next step, the learning interval is increased Δt.

Usually, the quality of the forecast is estimated by the percentage of detection of target events for a given average value of the alarm zone. Here, we consider a generalization of the method of minimum area of alarm, designed to improve another characteristic of the forecast quality: the probability of occurrence of at least one target event in the expected alarm zone. The difference between the methods is that at the moment of forecasting t^* two decisions are made: forecast in time and in space. The first solution determines the possibility of an earthquake epicenter with a target magnitude in the forecast interval. If it is decided that the target event is possible, then a map with an alarm zone is calculated. A target earthquake is predicted if its epicenter falls into the calculated alarm zone.

Predictive modeling is carried out for California. The initial data are earthquake catalog and GPS time series. The results showed rather high estimates of the probability of detecting target events and very small values of estimates of the probability of predicting the appearance of the epicenter of a target event in the alarm zone. At the same time, the estimates of the probability of a systematic forecast are much higher than the similar forecast probabilities for random fields.

Keywords: Earthquake forecast · Machine learning · Method of minimum area of alarm · Forecast quality · Spatio-temporal processes

The paper is supported by the Russian Science Foundation, project No20-07-00445.

© The Author(s), under exclusive license to Springer Nature Switzerland AG 2022
O. Gervasi et al. (Eds.): ICCSA 2022 Workshops, LNCS 13379, pp. 607–624, 2022.
https://doi.org/10.1007/978-3-031-10545-6_41

1 Introduction

Strong earthquakes cause great social and economic damage. Timely warning of a devastating earthquake can reduce loss of life and property damage. In this case, the damage from earthquakes is determined by the losses both from the destruction of the event missed during the forecast and from the implementation of protective measures in case of a false alarm.

The task of earthquake forecasting is usually to indicate an alarm zone limited in size, in which an earthquake epicenter with a magnitude greater than a certain threshold is expected within a certain time. Ideas about the possibility of predicting earthquakes are based on the data of physical modeling of the process of destruction of rocks and real observations, which show that an earthquake is preceded by processes that form anomalous changes in the geological environment in the area of the source of the expected earthquake [30–32]. So, for example, in the area of preparation for a strong earthquake, anomalous deviations were recorded in the frequency and strength of seismic events, in deformations of the earth's surface, in the chemical composition of fluids, in the level of groundwater, in the time of passage of seismic waves, in the magnitudes of the electric and geomagnetic fields, etc. [15,20,22,25,30,32]. This testifies in favor of the assumption that an earthquake can be predicted from local changes in the geological environment.

Earthquake forecasting works are being carried out in many directions. They include the study of rock destruction mechanisms, the study of various earthquake precursors, the development of mathematical models and forecasting methods. At the same time, there is an opinion that earthquake prediction is impossible [8,12,16]. The complexity of earthquake prediction is mainly due to two factors. Methods based on the physical features of the seismological and geodynamic regime require that the models of earthquake source preparation be determined by quantitative indicators available for instrumental measurements. Statistical forecasting methods require improvement of the network for monitoring seismic and geodynamic processes, increasing the types of instrumental observations, and increasing their accuracy.

Currently, machine learning methods are widely used for earthquake prediction [2,7,13,17,21,24,28,29]. In a number of works, artificial neural networks [1,23,27], as well as their hybrid and recurrent modifications [3,26], are used for forecasting. These methods require sufficiently large samples of target events for training. At the same time, it is known that for a number of seismically active regions, the number of strong seismic events during training intervals is small. Therefore, some simpler models may have similar or better predictive capabilities.

In this paper, we develop the approach to systematic earthquake prediction presented in [9–11]. A systematic prediction algorithm with a constant time step is regularly trained on occurred earthquakes and calculates a map of the alarm zone in which the target earthquake is expected. The alarm zone is determined by the function of the grid of spatio-temporal fields of features, calculated on the basis of the initial data. The approach is based on a machine learning method

called the method of the minimum area of alarm. During training, the method uses a mathematical model that allows you to identify anomalies in the feature fields preceding the target earthquakes, compare these anomalies with each other, and then highlight similar anomalies in the attribute fields during the forecast. This model introduces constraints on the prediction rule that help to compensate to some extent for the small number of strong earthquakes used for training.

In our previous works, the main characteristic of the quality of a systematic forecast was the proportion of detected earthquake epicenters with a target magnitude for a given value of the alarm zone. Here we consider a generalization of the method designed to improve one more characteristic of the forecast quality: the probability of the target event occurring in the selected time interval and in the zone of expected alarm. The main elements of the approach are presented in Sect. 2. In Sect. 3, the generalized method of the minimum alarm zone is considered. Sections 4 and 5 present the results of approbation of the earthquake prediction method on the seismological and geodynamic data of California.

2 Main Elements of the Approach

2.1 Formulation of the Problem

The fundamentals of the technology for an automatic system for systematic earthquake prediction were developed in 2018 [11]. A demo version of the system is available at https://distcomp.ru/geo/prognosis-gps/. Earthquake forecasts are given in increments of Δt. At each step, the selection of target earthquake epicenters is replenished from remote servers and new initial data on the seismic process are loaded. The data is processed, transformed into spatio-temporal fields of the grid of predictive features, and machine learning is performed on the data from the beginning of training until the prediction moment t^*. As a result, the alarm zone is calculated, in which the epicenter of the target earthquake is expected at the interval $(t^*, t^* + \Delta t]$. At the next step, the learning interval is increased by Δt.

The approach to systematic earthquake prediction is based on the method of minimum area of alarm. In [9–11], the quality of the forecast was estimated by the probability of detecting the epicenters of the target earthquakes, which was defined as the fraction of predicted target events. In this article, we generalize our method to bring the approach closer to practical applications. In the simplest case, it is important in practice to know the estimate of the probability of at least one target event falling into the calculated alarm zone. Let the forecast be given regularly with a step Δt, the number of forecasts N, and all target events in the analysis zone are contained in M intervals. Estimation of the probability of choosing an interval with a target event $P = M/N$. This value is an upper estimate of the probability that at least one target event will fall into the alarm zone within a given interval. In a number of seismically active regions, with a long-term forecast of strong earthquakes for relatively short time intervals Δt, the estimate of the probability P of forecasting the interval containing the target event is too small for making practical decisions about declaring an alarm.

This explains the need to develop an approach to the systematic prediction of earthquakes and to generalize the machine learning method.

The difference of the generalized method of the minimum area of alarm is that at the forecast moment t^* the algorithm makes two decisions. The first solution determines the possibility of an earthquake epicenter with a target magnitude in the analysis zone at the forecast interval $(t^*, t^* + \Delta t]$. This solution does not depend on the spatial position of the expected earthquake epicenter. Let's call this decision *time forecast*. If it is decided that a target event in the analysis zone is possible, then this time interval is declared an alarm interval, and the alarm zone is calculated on it. We will call this solution *spatial forecast*. A target earthquake is predicted if its epicenter falls within the calculated alarm zone. The more successful the forecast, the greater the product $s(t^*)\Delta t$. At the same time, it is obvious that the size of this spatio-temporal area should be reasonably limited in forecasting.

2.2 Model

We assume that, within the analysis zone, the precursors of occurred earthquakes may precede similar future earthquakes.

1. *Fields of forecast features*. The processes associated with the preparation of strong earthquakes can be represented by spatial and spatio-temporal grid fields. The field values at the grid nodes correspond to the vectors of the multidimensional feature space.
2. *Abnormality of features*. Strong earthquakes are preceded by anomalous values of grid fields close to maximum or minimum.
3. *Precursor cylinder*. The field grid node corresponding to a possible earthquake precursor is located in the cylinder preceding this earthquake, with the center of the base at the epicenter.
4. *Condition of monotonicity*. Let the vector $\mathbf{f}^{(q)}$ be a precursor of an earthquake q. Let the attribute fields be known, the anomalous values of which f_i^+ are close to the maximum, and the fields, the anomalous values of which f_i^- are close to the minimum. Then any vector $\mathbf{f}$, the values of whose components are equal to $f_i^+ \geq f_i^{(q)+}$ or $f_j^- \leq f_j^{(q)-}$, can also be a precursor of a similar event.

The monotonicity condition corresponds to the ideal situation when the fields of features contain complete information about earthquake preparation processes. In a real situation, this information is not complete. Therefore, for some earthquake precursors, the monotonicity condition is not satisfied. However, the monotonicity condition allows us to introduce a measure of the anomalousness of the earthquake precursor. This measure is used by the learning algorithm to find the prediction rule.

Further, in Sect. 2, to simplify the explanation of the method of minimum area of alarm, without loss of generality, we will assume that the anomalous components of earthquake precursors take only values of the fields of predictive features that are close to the maximum.

2.3 Generalized Method of the Minimum Area of Alarm

The method of the minimum area of alarm uses fields of spatio-temporal features and earthquake epicenters with target magnitudes for training. The training begins with the fact that the algorithm of the method finds anomalous values in the grid fields, which are further considered as possible earthquake precursors. As a result, the training sample set consists of vectors of earthquake precursors $\mathbf{f}^{(q)} = (f_1^{(q)}, f_2^{(q)}, \ldots, f_I^{(q)})$ and unlabeled vectors of values of the field $\mathbf{f}^{(g)}$ in all other nodes of the coordinate grid, among which there may be earthquake precursors not represented in the training set. Based on these data, in the learning process, it is required to learn how to determine the largest number of earthquake epicenters provided that the number of selected unmarked vectors is limited. Machine learning algorithms in this setting refer to one-class classification methods [5,14,18].

Let it be known that the event q is preceded by a precursor $\mathbf{f}^{(q)}$. Associated with the precursor is a set $w^{(q)}$ of vectors in the feature space $\mathbb{R}^I$ whose components are greater than or equal to $\mathbf{f}^{(q)}$, i.e., $w^{(q)} = \{\mathbf{f}^{(g)} \in \mathbb{R}^I \colon f_i^{(g)} \geq f_i^{(q)}, i = 1, 2, \ldots, I\}$. We call this set the orthant $w^{(q)}$ with vertex at the point $\mathbf{f}^{(q)}$, and the vectors $\mathbf{f}^{(g)} \in w^{(q)}$ as the *base vectors* of the target event q.

The basis vectors of the event q, according to the monotonicity condition, are also precursors of such events. In geographic coordinates, each base vector forms an *alarm cylinder* of radius R and element T. Each base vector forms, in geographic coordinates, an alarm cylinder of radius R and element T. The alarm cylinder of the base vector $\mathbf{f}^{(g)}$ has its base centered at grid node g with coordinates $(x(g), y(g), t(g))$, the radius of the base R and the element $[(x(g), y(g), t(g)), (x(g), y(g), t(g) + T)]$, where $t^{(g)} \in [t_0, t^*]$, t_0 is learning start time, t^* is the moment of prediction. An earthquake can only be predicted if its epicenter falls into one of the alarm cylinders. The union of the alarm cylinders formed by the base vectors of the orthant $w^{(q)}$, selects the set of grid nodes $W^{(q)}$, $|W^{(q)}| = L^{(q)}$. The learning algorithm uses the alarm cylinders to calculate the space-time alarm field.

Note now that an earthquake q with epicenter coordinates $(x(q), y(q), t(q))$ can fall into the alarm cylinder and, therefore, can be predicted if and only if its precursor $\mathbf{f}^{(q)}$ corresponds to some grid node from a cylinder with base center at point $(x(q), y(q), t(q))$, radius R and element $[(x(q), y(q), t(q) - T), (x(q), y(q), t(q))$. Let's call this cylinder the *cylinder of the precursor* of the event q. The precursor of the event q is the vector $\mathbf{f}^{(q)}$, which has the minimum value $v^{(q)} = L^{(q)}/L$ among all vectors corresponding to the nodes of the predecessor cylinder of the grid, where $|W^{(q)}| = L^{(q)}$, L is the number of all grid nodes of the spatio-temporal area of analysis on the interval $[t_0, t^*]$. The value $v^{(q)}$ (the *volume of the precursor*) determines the measure of the anomaly of the precursor of the event q.

The scheme of the learning algorithm for the method of the generalized minimum area of alarm is as follows. The forecast of the target event at the moment t^* of the interval $(t^*, t^* + \Delta t]$ is carried out in two stages. At the 1st stage, the problem of choosing the time interval for the forecast is solved, at which the

target event is expected within the analysis zone. If it is decided that the target event is possible at this interval, then the 2nd stage of the forecast is performed: the problem of determining the alarm zone in which the target event is expected is solved.

Stage 1: Forecast in Time. At the 1st stage, the radius of the cylinders R is chosen so that the circle centered at any grid node of the analysis area covers the entire analysis area. This leads to the fact that the earthquake precursor can refer to any grid node of the analysis area. Thus, the precursor loses its spatial localization and the alarm cylinder degenerates into an alarm time interval, and the space-time alarm field degenerates into an alarm time series Ψ.

The algorithm for calculating the time series of alarms for the time t^* is as follows.

1. Find earthquake precursors $\mathbf{f}^{(q)}$ for each target event $q = 1, 2, \ldots, Q$. Let the event q occur at the moment $t^{(q)}$. The precursor $\mathbf{f}^{(q)}$ of the event q is sought on the interval $[t^{(q)} - T, t^{(q)})$ among the vectors corresponding to the grid nodes $g = 1, 2, \ldots, G$ of the precursor cylinder. Each of these vectors $f^{(g)}$ selects the orthant $w^{(g)}$ of base vectors and selects a set of samples of the time series of signals $W^{(g)}$, $|W^{(g)}| = N^{(g)}$. The precursor of the event q is the vector $\mathbf{f}^{(q)}$ with the minimum volume of the precursor $v^{(q)} = N^{(q)}/N$ among the vectors corresponding to the grid nodes of the precursor cylinder, where $N^{(q)}$ is the number of signal intervals when choosing the orthant $w^{(q)}$ with vertex $\mathbf{f}^{(q)}$, N is the number of all intervals from the beginning of training to the moment t^*.
2. Sort all the precursors $\mathbf{f}^{(q)}$ by increasing their alarm volume: $v^{(1)} \le v^{(2)} \le \cdots \le v^{(q)} \le \cdots \le v^{(q)}$.
3. Calculate the alarm time series Ψ.
   (a) Set the values $\psi(t) \equiv 1$.
   (b) Replace the values 1 to the value $\psi(1) = v^{(1)}$ in the set $W^{(1)}$; replace the value 1 with the value $\psi(2) = |W^{(1)} \cup W^{(2)}|/N$ in the set $W^{(2)} \setminus W^{(1)}$; replace the value 1 with the value $\psi(3) = |W^{(1)} \cup W^{(2)} \cup W^{(3)}|/N$ in the set $W^{(3)} \setminus (W^{(1)} \cup W^{(2)})$ and then sequentially replace the values 1 with the corresponding values of alarm volumes. The resulting alarm time series Ψ takes the values $\psi(1) \le \psi(2) \le \cdots \le \psi(q) \le \cdots \le \psi(Q) \le 1$.

Thus, at the forecast moment t^*, the values of the time series Ψ are updated. The decision to declare an alarm on the interval $(t^*, t^* + \Delta t]$ is made if $\psi(t^*) \le \psi_0$, where ψ_0 is the value of the specified threshold. Intervals Δt of a series of alarms Ψ with sample values $\psi(t^*) \le \psi_0$ will be called alarm intervals. The number M^* of detected alarm intervals with target events, depends on the value $\Psi = N^*/N$, where N^* is the number of alarm intervals, N is the total number of all forecast intervals. The quality of the forecast at the 1st stage is determined by the following statistics: $U^* = M^*/M$ is an estimate of the probability of successful detection of an interval in which at least one target event occurred, where M is the number of all intervals containing at least one target event, and

$P_1 = M^*/N^*$ is an estimate of the probability that at least one target event will occur in the predicted alarm interval.

Stage 2: Spatial Forecast. The spatial forecast defines alert zones where target earthquakes are expected. Alarm zones are calculated only on alarm intervals with values $\psi(t^*) \le \psi_0$. In this case, as in the previous stage, all data available by the time of forecasting t^* are used for training: grid fields $\mathbf{F}_1, \mathbf{F}_2, \ldots, \mathbf{F}_I$ and target events $q = 1, 2, \ldots, Q$.

The learning algorithm uses the following parameters:

1. The area of analysis and the time step of the coordinate grid do not change compared to the 1st stage.
2. The grid of spatial coordinates is determined by the accuracy of the data.
3. The parameters of the signal and precursor cylinders are the same and depend on the accuracy of the data, the grid spacing, and the features of regional seismicity.

The alarm field calculation algorithm consists of three steps:

1. Calculate earthquake precursor vectors $\mathbf{f}^{(q)}$, $q = 1, \ldots, Q$ (see previous section)
2. Generate training sample $\{f^{(q)}, v^{(q)}\}$. Order cases $f^{(q)}$ by increasing volume of alarms for the target event $v^{(1)} \le v^{(2)} \le \cdots \le v^{(q)} \le \cdots \le v^{(Q)}$.
3. Calculate the alarm field Φ.
   (a) Set the grid nodes of the alarm field to 1.
   (b) Replace the value 1 of the field Φ with $\phi(1) = v^{(1)}$ for the set $W^{(1)}$ of grid nodes corresponding to the base points of $\mathbf{f}^{(1)}$; replace the value 1 with $\phi(2) = |W^{(1)} \cup W^{(2)}|/L$ at the grid nodes, $W^{(2)} \setminus W^{(1)}$; replace value 1 with $\phi(3) = |W^{(1)} \cup W^{(2)} \cup W^{(3)}|/L$ at grid nodes $W^{(3)} \setminus (W^{(1)} \cup W^{(2)})$, and then sequentially replace the values of 1 with the corresponding alarm volume values. The resulting field Φ takes the values $\phi(1) \le \phi(2) \le \cdots \le \phi(q) \le \cdots \le \phi(Q) \le 1$.

Thus, at each step of the forecast Δt, new values of the spatio-temporal alarm field Φ are calculated. The time interval of the alarm field at time t^* is used for prediction. The decision on the success of the forecast of an earthquake with a target magnitude on the interval $(t^*, t^* + \Delta t]$ is made if its epicenter falls into the alarm zone $\phi(t^*) \le \phi_0$, where ϕ_0 is the value of the specified threshold. The number of events M^{**} in the alarm zones, calculated in the alarm intervals selected at the 1st stage, depends on the value of the alarm volume $\phi_0 = L^*/L$, where L^* is the average number of grid nodes in the signal zones, L is the total number of grid nodes in the analysis zone for all intervals Δt on which the forecast decision was made. The quality of the forecast at the 2nd stage is determined by the following statistics: $U^{**} = Q^{**}/Q$ is the estimate of the probability of successful detection of the target event at alarm intervals, where M is the number of intervals with the target event in the analysis zone, M^{**} is the number of alarm intervals with target events in the alarm zone, and $P2 = M^{**}/N^*$ is an estimate of the probability that at least one target event that falls into the alarm interval will also fall into the predicted alarm zone.

3 Modeling

3.1 Initial Data

Earthquake prediction modeling was performed on data from the California region. The initial data include the earthquake catalog of the National Earthquake Information Center (NEIC) [4] for 01/01/1995–11/14/2020 with magnitude $m \geq 2.0$ and hypocenter depth $H \leq 160$ km, as well as GPS time series of daily horizontal displacements of the earth's surface in the interval 01/01/2008–11/14/2020 from the Nevada Geodetic Laboratory (NGL), http://geodesy.unr.edu/about.php [6]. The average distance between GPS receiving stations is 9.38 km, with a standard deviation of 5.74 km. The forecast is calculated for earthquake epicenters with target magnitude $m \geq 5.5$ and hypocenter depth $H \leq 60$ km. The analysis zone is defined by the intersection of two zones. The first zone is calculated from seismological data. The zone is limited by the threshold spatial density of earthquake epicenters in the interval 1995–2008, at which, for the alarm volume $\phi_0 = 0.2$, the probability of detecting earthquake epicenters with magnitude $m \geq 5.5$ in this field will not exceed 0.3–0.4. The second zone is limited to an area for which the distance to the ground receiving GPS stations does not exceed 50 km. The area of analysis is shown in Fig. 1. The circles show the epicenters of target earthquakes with magnitude $m \geq 5.5$ used for training (yellow) and forecast (red).

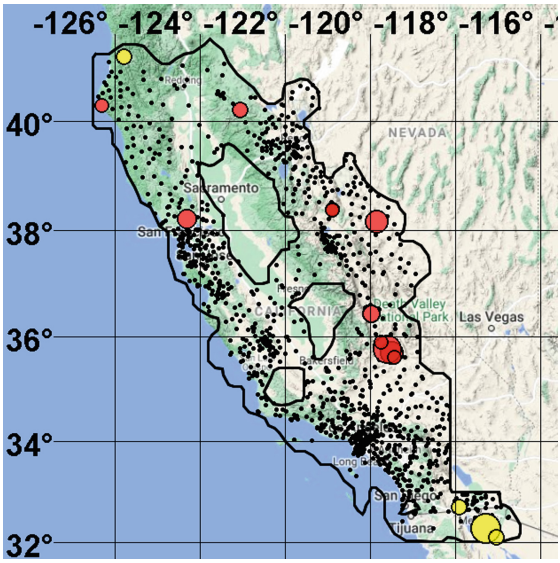

Fig. 1. Zone of analysis. Circles are epicenters of target earthquakes with magnitudes $m \geq 5.5$ used for training (yellow) and testing (red). Black dots are GPS receiving stations. (Color figure online)

3.2 Preprocessing

Seismological Data. are presented in the form of the following main spatial and spatio-temporal grid fields, similar to those used in our previous works [9–11]:

1. $\mathbf{S}_1$ is the 3D density field of earthquake epicenters.
2. $\mathbf{S}_2$ is the 3D field of medium magnitude earthquakes.
3. $\mathbf{S}_3$ is the 3D field of variations in the density of earthquake epicenters over time. The values of the field $s_{3n}(t)$ at grid node n are equal to the ratio of the difference between the average values of the density of epicenters $(\overline{s_{1n}} - \overline{s_{2n}})$ in two successive intervals T_1 and T_2 to the sample standard deviation of this difference $\sigma_n(s_1)$.
4. $\mathbf{S}_4$ is the 3D field of variations of mean magnitudes of earthquakes over time. The field values are calculated similarly to the values of the $\mathbf{S}_3$ field,
5. $\mathbf{S}_5$ is the 3D field of quantiles of the background density of earthquake epicenters in the interval from the beginning of the analysis to the start of training, the values of which correspond to the density of earthquake epicenters in the analysis interval.
6. $\mathbf{S}_6$ is the 2D density field of earthquake epicenters in the interval from the beginning of the analysis to the start of training.

When choosing the most informative fields of features, in addition to the fields indicated in the list, fields equal to their products and ratios were used.

Geodynamic Data. are presented as time series of the $x(t)$ and $y(t)$ components of the coordinates of daily horizontal displacements of GPS receiving stations in the west-east and north-south directions. The efficiency of using space geodesy data for earthquake prediction was studied in [10]. Calculation of fields from GPS time series is performed in two stages. At the first stage, a useful signal is extracted from the time series of GPS receiving stations, then the space-time fields of prognostic features are calculated.

The daily displacement velocity of the earth's surface $g_x(t)$ and $g_y(t)$ are calculated over the interval $T_0 = 30$ days: $g_x(t) = (x(t) - x(t - T_0))/T_0$ and $g_y(t) = (y(t) - y(t - T_0))/T_0$. Changes in the $x(t)$ and $y(t)$ station coordinates over a thirty-day interval are comparable to the measurement noise. For each coordinate of the time series, there are a large number of discontinuities. If after each break you start counting the speed again, then the number of missing values increases significantly. To limit the number of gaps in the time series of velocities, we linearly interpolate the values of the station coordinates at discontinuities not larger than T_0. When the breaks in the series of coordinates are more than T_0, we end the calculation of the speed at the last value before the break and again continue estimating the speeds, starting from the first value after the break.

Spatio-temporal fields are calculated in the grid $\Delta x \times \Delta y \times \Delta t = 0.1^\circ \times 0.075^\circ \times 1$ day. Time series values are interpolated using the well-known method of weighted inverse distances. As a result of interpolation, the gaps in the velocity

time series related to the nodes of the spatial grid are filled with data from neighboring receiving stations. After field interpolation, the velocity components $\mathbf{V}_x$ and $\mathbf{V}_y$ were spatially smoothed with a sliding window of 25×25 km^2.

We assume that the precursors of strong earthquakes can be detected in spatio-temporal fields of anomalous changes in the mode of deformations of the earth's surface. Anomalies in time were calculated in three fields of strain rate invariants:

- $\mathbf{F}_1$ is the strain rate divergence field: $\operatorname{div} V_g = \frac{\partial V_{xg}}{\partial x} + \frac{\partial V_{yg}}{\partial y}$
- $\mathbf{F}_2$ is the rotor strain rate field: $\operatorname{rot} V_g = \frac{\partial V_{xg}}{\partial y} - \frac{\partial V_{yg}}{\partial x}$
- $\mathbf{F}_3$ is the field of shear deformations: $\operatorname{sh} V_g = \frac{1}{2}\sqrt{(\frac{\partial V_{xg}}{\partial x} - \frac{\partial V_{yg}}{\partial y})^2 + (\frac{\partial V_{xg}}{\partial y} + \frac{\partial V_{yg}}{\partial x})^2}$
- $\mathbf{F}_4$ is the field of variations in the strain rate divergence. The values of the field $f_{4g}(t)$ at the grid node g are equal to the ratio of the difference between the average divergence values $(\overline{div_{2g}} - \overline{div_{1g}})$ in two successive intervals T_1 and T_2 to the standard deviation of this difference $\sigma_g(div)$, where $T_1 = T_2 = 361$ days and $\overline{div_{2g}}$ is calculated from the values of the field $\mathbf{F}_1$ on the interval $(t - T_2, t)$, $\overline{div_{1g}}$ is calculated on the interval $(t - T_2 - T_1, t - T_2)$.
- $\mathbf{F}_5$ is the field of variations of the rotor deformation rate. The values of the field f5(t) are calculated similarly to the values of the field $\mathbf{F}_4$, $f_{5g}(t) = (\overline{rot2g} - \overline{rot_{1g}})/\sigma_g(rot)$.
- $\mathbf{F}_6$ is the field of shear strain variations: $f_{6g}(t) = (\overline{sh2g} - \overline{sh_{1g}})/\sigma_g(sh)$.

The fields $\mathbf{F}_4$, $\mathbf{F}_5$, $\mathbf{F}_6$ were calculated in the coordinate grid $\Delta x \times \Delta y \times \Delta t = 0.1^\circ \times 0.075^\circ \times 30$ days.

3.3 Forecast

Detection of Target Events. The following forecast parameters were used. The training interval starts on September 23, 2009 and ends at the time of the next forecast. The forecast is performed regularly with a step of $\Delta t = 30$ days in the testing interval until 11/14/2020. During the test period, 12 epicenters of earthquakes with magnitude $m \geq 5.5$ fall into the analysis zone. The parameters of the alarm and precursor cylinders are $R = 18$ km and $T = 61$ days. To calculate the alarm field, the same 4 fields were used as in the article [10]: (1) field $\mathbf{F}_6$—maximum values of variations in time of shear deformations of the earth's surface with parameters $T_1 = T_2 = 365$ days; (2) field $\mathbf{F}_4$—the maximum values of variation in time of divergence of the earth's surface with parameters $T_1 = T_2 = 365$ days; (3) field $\mathbf{S}_{12}$ - minimum values of variations in the field $\mathbf{S}_2$ of average magnitudes of earthquakes in time with parameters $T_1 = 1095$ and $T_2 = 730$ days; (4) field $\mathbf{S}_{13} = \mathbf{S}_1/\mathbf{S}_5$—ratios of the density values of earthquake epicenters in field $\mathbf{S}_1$ and quantiles in field $\mathbf{S}_5$. For comparison, the forecast was calculated from the $\mathbf{S}_6$ fields of the spatial density of earthquake epicenters. The main results are shown in Fig. 2 and summarized in Table 1.

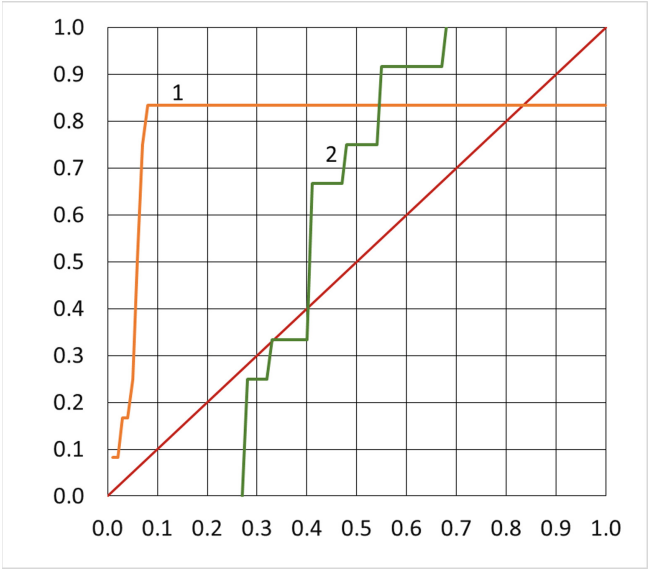

Fig. 2. Plot $U(\phi)$ of the probabilities of detecting target events U on the alarm volume ϕ: 1—forecast for the selected spatio-temporal fields, 2—forecast for the spatial density field of earthquake epicenters.

Table 1. Probability of detecting target events.

Alarm volume threshold ϕ	Fields F_4, F_6, S_{12} and S_{13}		Field of 2D earthquake density S_6	
	Number of Events Q^*	Probability $U = Q^*/Q$	Number of Events Q^*	Probability $U = Q^*/Q$
0.05	3	0.39	0	0
0.10	10	0.83	0	0
0.15	10	0.83	0	0
0.20	10	0.83	0	0
0.25	10	0.83	0	0
0.30	10	0.83	3	0.25

It can be seen from the figure and tables that the values of the probability of detecting target events when using the indicated spatio-temporal fields are much higher than when using the spatial density field of earthquake epicenters. This indicates the spatial homogeneity of target events in the selected areas of analysis.

The California testing interval 01/19/2013–11/14/2020 contains $N = 95$ forecast intervals Δt. All target events $Q = 12$ with magnitude $m \geq 5.5$ fall within the forecast intervals $M = 7$. The number of alarm intervals for which target events falls into zones with alarm volume $\phi = 0.2$ is equal to $M^{**} = 6$. The estimate of the probability that in the forecast interval Δt at least one target event will fall into the analysis zone is equal to the proportion of forecast intervals with target events $P = M/N = 7/95 = 0.07$.

Stage 1. At the 1st stage, the alarm interval is selected, during which the target event is expected in the analysis zone. The values of spatio-temporal fields calculated from GPS data for the California region are known for a very short interval of 09/23/2009–11/14/2020. This entire interval was used for testing.

Feature fields were spatially smoothed with a 200 km radius window and converted to a grid $\Delta x \times \Delta y \times \Delta t = 1.85° \times 1.85° \times 30$ days. The temporal forecast was made using two fields: (1) field $F_{6smoothed}$—the maximum values of the field of variations in shear deformations of the earth's surface in time with parameters $T_1 = T_2 = 365$ days; (2) field $F_{4smoothed}$—the minimum values of the field of variations in the divergence of the earth's surface in time with the parameters $T_1 = T_2 = 365$ days. Parameters of the minimum alarm zone algorithm: $T = 61$ days, $R = 3000$ km. The decision to assign a forecast interval as an alarm interval is made if the values of the time series Ψ do not exceed the threshold value $\psi_0 = 0.35$.

Figure 3 shows the dependence of the probability estimate $U^* = M^*/M$ of detecting test earthquakes in alarm intervals Δt on the proportion of alarm intervals $\psi = N^*/N$, where N^* is the number of alarm intervals, N is the number of all predictive intervals, M is the number of all alarm intervals with target events, M^* is the number of alarm intervals in which target events are present, P_1 is the probability that at least one target event falls into the analysis zone during the alarm interval. Figure 4 shows a plot of the alarm time series Ψ and the sequence of target earthquakes in the testing interval.

The Table 2 shows that the threshold $\psi_0 = 0.35$ corresponds to the estimate of the probability of hitting at least one target event in the analysis zone during the alarm interval $P1 = M^*/N^* = 7/41 = 0.17$. The value P_1 is the upper limit for estimating P_2 the probability that at the 2nd stage at least one target event will fall into the alarm zone of one of the N^* alarm intervals selected at the first stage.

Table 2. Testing the 1st stage of the forecast.

Alarm volume threshold ϕ	N^*	M^*	$U^* = M^*/M$	$P_2 = M^*/N^*$
0.25	30	5	0.71	0.17
0.45	41	7	1.00	0.17

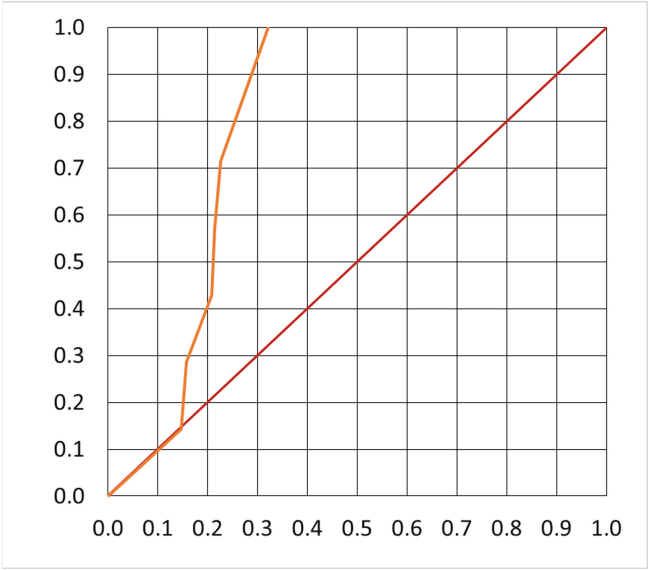

Fig. 3. Graphs of dependence $U^*(\psi)$.

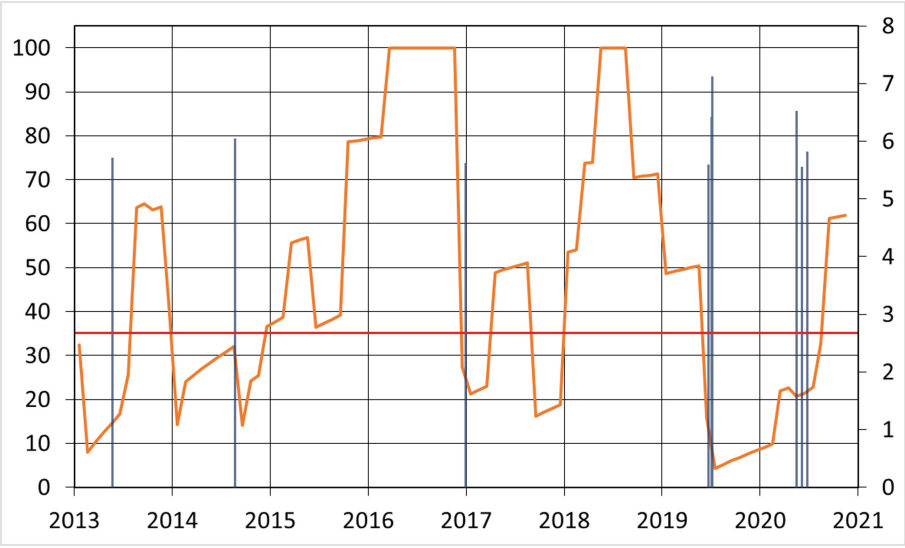

Fig. 4. Time series of alarm intervals Ψ and test sequence of target earthquakes with $m \geq 5.5$. The decision to alarm is made if the values of the time series do not exceed the value $\psi_0 = 0.35$.

Stage 2. For spatial forecasting, the same fields were used as in the "Target Event Detection" section. The results of modeling the 2nd stage of the forecast are summarized in Table 3. The following designations are used in the table: $\phi = L^*/L$ is the average proportion of alarm grid nodes relative to the analysis zone; N^* is the number of selected alarm intervals during testing; $M^{**}(\psi_0, \phi_0)$ is the number of alarm intervals in which at least one target event fell into the alarm zone during testing; $U^{**} = M^{**}(\psi_0, \phi_0)/M$ is an estimate of the probability of detecting alarm intervals for which at least one target event fell into the alarm zone; $P_2 = M^{**}(\psi_0, \phi_0)/N^*(\psi_0)$ is the estimate of the probability of at least one target event falling into the alarm zone in the alarm interval.

Table 3. Testing the 2nd stage of the forecast.

Alarm volume threshold ϕ	M^{**}	U^{**}	P_2
0.10	6	0.86	0.15
0.20	6	0.86	0.15
0.30	6	0.86	0.15

It can be seen from the table that at the threshold $\psi_0 = 0.35$, starting from the threshold $\phi_0 = 0.1$, $U^{**} = 0.86$ and $P_2 = 0.15$.

4 Discussion

The modeling results can be summarized with the following four metrics:

1. Estimate of the probability of detecting target events U for a given volume of alarm ϕ, equal to the proportion of detected events Q^* in predictive alarm zones, the area of which, on average, from the beginning of training to the moment of forecasting, is part ϕ_0 of the area of the analysis zone: $U = Q^*(\phi_0)/Q$.
2. Estimate of the probability of detecting alarm intervals with target events M* for a given share of alarm intervals ψ_0 from all intervals M: $U^* = M^*(\psi_0)/M$.
3. Estimation of the probability of occurrence of at least one target event at the predicted alarm interval Δt in the analysis zone (probability of the forecast in time): $P_1 = M^*(\psi_0)/N^*(\psi_0)$.
4. Estimation of the probability of occurrence of at least one target event at the signal interval Δt in the predicted alarm zone (spatio-temporal probability of the forecast): $P_2(\psi_0, \phi_0) = M^{**}(\psi_0, \phi_0)/N^*(\psi_0)$.

For comparison, we will use the values of the same indicators when predicting target events for random fields.

1. The probability of detecting target events when choosing an alarm zone by a random field with an alarm volume ϕ: $U_{rand}(\phi) = \phi = L^*/L$.

2. Probability of detecting alarm intervals Δt with target events when choosing N^* intervals from N random field values: $U^*_{rand}(\psi) = \psi = N^*/N$.
3. The probability that, under the condition of a uniform distribution of intervals Δt with target events, a randomly selected interval will contain at least one target event: $P_{1rand} = M/N$.
4. Probability P_{2rand} that, with a random selection of the alarm zone, at least one of the target events, provided that they are evenly distributed in the analysis zone, will appear in the randomly generated alarm zone. Let X be a random variable equal to the number of events in the alarm zone. The average value $\overline{X} = \phi Q/N$, where the alarm volume ϕ is equal to the ratio of the average value of the area of the alarm zone to the area of the analysis zone, the number of intervals N is equal to the ratio of the testing time to the value of the forecast interval Δt. Assuming that the empirical mean X is equal to the mathematical expectation $\mathrm{E}\,X$, one can estimate P_{2rand} using the Markov inequality [19]: $P_{2rand}(X \geq 1) \leq \phi Q/N$.

Table 4 compares the results of a systematic earthquake forecast and the results of a forecast based on random fields.

Table 4. Results of systematic and random forecasts.

№	Indicator	Systematic forecast	Random forecast
1	Detection of target events $U(\phi) = Q^*(\phi)/Q$	$U(0.10) = 10/12 = 0.83$ $U(0.20) = 10/12 = 0.83$ $U(0.30) = 10/12 = 0.83$	$U_{rand}(\phi) = \phi = 0.10$ $U_{rand}(\phi) = \phi = 0.20$ $U_{rand}(\phi) = \phi = 0.30$
2.	Detection of intervals with events $U^*(\psi) = M^*(\psi)/M$	$U^*(0.25) = 5/7 = 0.71$ $U(0.35) = 7/7 = 1.00$	$U_{rand}(\psi) = \psi = 0.25$ $U_{rand}(\psi) = \psi = 0.35$
3.	Interval prediction with target events $P_1(\psi) = M^*(\psi)/N^*(\psi)$	$P_1(0.25) = 5/30 = 0.17$ $P_1(0.35) = 7/41 = 0.17$	$P_{1rand} = M/N = 7/95 = 0.07$
4.	Forecast of target events $P_2(\phi, \psi) = M^{**}(\phi)/N^*(\psi)$	$P_2(0.2, 0.35) = 6/41 = 0.15$ $P_2(0.3, 0.35) = 6/41 = 0.15$	$P_{2rand} \leq \phi Q/N = 0.2 \times 12/95 = 0.03$ $P_{2rand} \leq \phi Q/N = 0.3 \times 12/95 = 0.04$

The results show that with a systematic forecast, the estimates of the probability of detecting target events $U(\phi)$ and alarm intervals with events $U^*(\psi)$ take quite high values. However, for the practical application of earthquake prediction methods, it is more important to estimate the forecast probabilities $P_1(\psi)$ and $P_2(\psi, \phi)$, the probability of at least one target event occurring in the predicted alarm intervals and the alarm zone. It can be seen that the experimental estimates of these values take small values. At the same time, these estimates of forecast probabilities are higher than similar values obtained when using random attributive fields for forecasting, and also higher than those obtained in section "Detection of target events", when using the previous version of the minimum alarm zone method: $P_1 = 0.07$ at $\psi_0 = 0.35$ and $P_2 = 0.06$ at $\phi_0 = 0.2$.

5 Conclusion

We have considered the main elements of the approach to systematic earthquake prediction. The forecast decision is made regularly for the time interval Δt. We determine the quality of the forecast using two types of estimates. We estimate: (1) the probability of detecting target events, which is equal to the share of detected events in the forecast, and (2) the probability of predicting target events, which determines the measure of the possibility of a target event occurring at the next alarm interval Δt in the analysis zone and in the predicted alarm zone. The predictive decision is made regularly for the time interval Δt. The first assessment determines the effectiveness of the initial data, methods of their processing, and the method of forecasting. The second assessment is necessary for making practical decisions related to seismic hazard prediction.

The solution to the second problem required the development of the method of minimum area of alarm. The generalized method consists of two steps. At the first stage, the possibility of an earthquake epicenter with a target magnitude in the analysis zone is predicted, and a decision is made to announce an alarm at the interval Δt. At the second stage, in the alarm interval, the spatial position of the alarm zone is calculated, in which the appearance of the epicenter of this earthquake is expected.

This method has been experimentally investigated for the California region. The forecast of earthquakes with magnitude $m \geq 5.5$ was made according to the catalog of earthquakes and time series of displacements of the earth's surface obtained using GPS. The simulation results show that for alarm zones, the area of which on average is from 10% of the area of the analysis zone, the estimates of the probability of detecting target events are more than 0.8. At the same time, the probabilities that at least one target earthquake is expected in the predicted alarm zone take on a very small order of magnitude, less than 0.15. At the same time, it can be seen that estimates of the probability of a systematic forecast are significantly higher than similar forecast probabilities based on random fields.

We believe that in order to develop an approach to systematic earthquake prediction in the direction of solving applied problems, it is advisable to conduct research on optimizing the method of systematic earthquake prediction and studying new grid fields representing the processes of preparation of sources of strong earthquakes.

Acknowledgements. This work was partially supported by RFBR grant 20-07-00445. The authors are grateful to E.N. Petrova and S.A. Pirogov for their helpful remarks.

References

1. Alves, E.I.: Earthquake forecasting using neural networks: results and future work. Nonlinear Dyn. **44**(1), 341–349 (2006)
2. Amei, A., Fu, W., Ho, C.H.: Time series analysis for predicting the occurrences of large scale earthquakes. Int. J. Appl. Sci. Technol. **2**(7) (2012)

3. Asim, K.M., Idris, A., Iqbal, T., Martínez-Álvarez, F.: Earthquake prediction model using support vector regressor and hybrid neural networks. PLoS ONE **13**(7), e0199004 (2018)
4. Barnhart, W.D., Hayes, G.P., Wald, D.J.: Global earthquake response with imaging geodesy: recent examples from the USGS NEIC. Remote Sens. **11**(11), 1357 (2019)
5. Bishop, C.M.: Machine learning and pattern recognition. In: Information Science and Statistics. Springer, Heidelberg (2006). ISBN:978-1-4939-3843-8
6. Blewitt, G., Hammond, W.C., Kreemer, C.: Harnessing the GPS data explosion for interdisciplinary science. Eos **99**(10.1029), 485 (2018)
7. Corbi, F., et al.: Machine learning can predict the timing and size of analog earthquakes. Geophys. Res. Lett. **46**(3), 1303–1311 (2019)
8. Geller, R.J., Jackson, D.D., Kagan, Y.Y., Mulargia, F.: Earthquakes cannot be predicted. Science **275**(5306), 1616 (1997)
9. Gitis, V., Derendyaev, A.: The method of the minimum area of alarm for earthquake magnitude prediction. Front. Earth Sci. **8**, 482 (2020)
10. Gitis, V., Derendyaev, A., Petrov, K.: Analyzing the performance of GPS data for earthquake prediction. Remote Sens. **13**(9), 1842 (2021)
11. Gitis, V.G., Derendyaev, A.B.: Machine learning methods for seismic hazards forecast. Geosciences **9**(7), 308 (2019)
12. Gufeld, I.L., Matveeva, M.I., Novoselov, O.N.: Why we cannot predict strong earthquakes in the earth's crust. Geodyn. Tectonophys. **2**(4), 378–415 (2015)
13. Keilis-Borok, V., Soloviev, A.A.: Nonlinear dynamics of the lithosphere and earthquake prediction. Springer Science & Business Media (2013)
14. Khan, Shehroz S.., Madden, Michael G..: A survey of recent trends in one class classification. In: Coyle, Lorcan, Freyne, Jill (eds.) AICS 2009. LNCS (LNAI), vol. 6206, pp. 188–197. Springer, Heidelberg (2010). https://doi.org/10.1007/978-3-642-17080-5_21
15. King, C.Y.: Gas geochemistry applied to earthquake prediction: an overview. J. Geophys. Res. Solid Earth **91**(B12), 12269–12281 (1986)
16. Koronovsky, N., Naimark, A.: Earthquake prediction: is it a practicable scientific perspective or a challenge to science? Mosc. Univ. Geol. Bull. **64**(1), 10–20 (2009)
17. Kossobokov, V., Shebalin, P.: Earthquake prediction. In: Nonlinear Dynamics of the Lithosphere and Earthquake Prediction, pp. 141–207. Springer (2003). https://doi.org/10.1007/978-3-662-05298-3
18. Kotsiantis, S.B., Zaharakis, I., Pintelas, P.: Supervised machine learning: a review of classification techniques. Emerg. Artif. Intell. Appl. Comput. Eng. **160**, 3–24 (2007)
19. Kremer, N.S.: Probability theory and mathematical statistics. YUNITI-DANA, M p. 573 (2004)
20. Lighthill, J.: A critical review of VAN: earthquake prediction from seismic electrical signals. World scientific (1996)
21. Marzocchi, W., Zechar, J.D.: Earthquake forecasting and earthquake prediction: different approaches for obtaining the best model. Seismol. Res. Lett. **82**(3), 442–448 (2011)
22. Matsumoto, N., Koizumi, N.: Recent hydrological and geochemical research for earthquake prediction in Japan. Nat. Hazards **69**(2), 1247–1260 (2013)
23. Mignan, A., Broccardo, M.: Neural network applications in earthquake prediction (1994–2019): meta-analytic and statistical insights on their limitations. Seismol. Res. Lett. **91**(4), 2330–2342 (2020)

24. Moustra, M., Avraamides, M., Christodoulou, C.: Artificial neural networks for earthquake prediction using time series magnitude data or seismic electric signals. Expert Syst. Appl. **38**(12), 15032–15039 (2011)
25. Murai, S.: Can we predict earthquakes with GPS data? Int. J. Digital Earth **3**(1), 83–90 (2010)
26. Panakkat, A., Adeli, H.: Neural network models for earthquake magnitude prediction using multiple seismicity indicators. Int. J. Neural Syst. **17**(01), 13–33 (2007)
27. Priambodo, B., Mahmudy, W.F., Rahman, M.A.: Earthquake magnitude and grid-based location prediction using backpropagation neural network. Knowl. Eng. Data Sci. **3**(1), 28–39 (2020)
28. Rhoades, D.A.: Mixture models for improved earthquake forecasting with short-to-medium time horizons. Bull. Seismol. Soc. Am. **103**(4), 2203–2215 (2013)
29. Shebalin, P.N., Narteau, C., Zechar, J.D., Holschneider, M.: Combining earthquake forecasts using differential probability gains. Earth, Planets and Space **66**(1), 1–14 (2014). https://doi.org/10.1186/1880-5981-66-37
30. Sobolev, G.: Principles of earthquake prediction (1993)
31. Sobolev, G., Ponomarev, A.: Earthquake physics and precursors. Publishing house Nauka, Moscow.-2003 (2003)
32. Zavyalov, A.: Intermediate term earthquake prediction. Nauka, Moscow. In: Zhang, L.Y., Mao, X.B., Lu, A.H. (eds.) (2009) Experimental Study of the Mechanical Properties of Rocks at High Temperature, Sci. China Ser. E, vol. 52(3), pp. 641–646 (2006)